

Published in final edited form as:

Bioorg Med Chem. 2013 March 1; 21(5): 1123–1135. doi:10.1016/j.bmc.2012.12.043.

Secondary Amines Containing One Aromatic Nitro Group: Preparation, Nitrosation, Sustained Nitric Oxide Release, and the Synergistic Effects of Released Nitric Oxide and an Arginase Inhibitor on Vascular Smooth Muscle Cell Proliferation

Brandon Curtis^a, Thomas J. Payne^b, David E. Ash^a, and Dillip K. Mohanty^{a,*}

^aDepartment of Chemistry, Central Michigan University, Mt. Pleasant, MI-48858, USA

Abstract

Atherosclerosis, a leading cause of death worldwide, is associated with the excessive proliferation of vascular smooth muscle cells. Nitrogen monoxide, more commonly known as nitric oxide, inhibits this uncontrolled proliferation. Herein we report the preparation of two families of nitric oxide donors; beginning with the syntheses of secondary amine precursors, obtained through the reaction between two equivalents of various monoamines with 2,4 or 2,6-difluoronitrobenzene. The purified secondary amines were nitrosated then subjected to a Griess reagent test to examine the slow and sustained nitric oxide release rate for each compound in both the absence and presence of reduced glutathione. The release rate profiles of these two isomeric families of NO-donors were strongly dependent on the number of side chain methylene units and the relative orientations of the nitro groups with respect to the N-nitroso moieties. The nitrosated compounds were then added to human aortic smooth muscle cell cultures, individually and in tandem with S-2-amino-6-boronic acid (ABH), a potent arginase inhibitor. Cell viability studies indicated a lack of toxicity of the amine precursors, in addition to anti-proliferative effects exhibited by the nitrosated compounds, which were enhanced in the presence of ABH.

Keywords

Sustained Nitric Oxide Release; Cell Culture Study; Smooth Muscle Cell Proliferation Inhibition

1. Introduction

The small gaseous molecule nitrogen monoxide, commonly known as nitric oxide (NO), is produced *in vivo* from L-arginine, and serves as a multifunctional signaling molecule. The production of NO, a radical species, (and L-citrulline) is catalyzed by nitric oxide synthases (NOS) (three isoforms of which are known), in the presence of additional co-factors. This same arginine pool also serves as the substrate for the *in vivo* production of ornithine catalyzed by arginase. Ornithine serves as the precursor to the subsequent syntheses of various polyamines (Fig. 1). [1–3] Though structurally simple, the complex role of NO in

© 2013 Elsevier Ltd. All rights reserved.

*Corresponding author. Tel.: +01 989 774 6445; Fax: +01 989 774 3883, Mohan1dk@cmich.edu.

^bPresent Address: Department of Biochemistry, University of TN, Knoxville, TN-37901, USA

Publisher's Disclaimer: This is a PDF file of an unedited manuscript that has been accepted for publication. As a service to our customers we are providing this early version of the manuscript. The manuscript will undergo copyediting, typesetting, and review of the resulting proof before it is published in its final citable form. Please note that during the production process errors may be discovered which could affect the content, and all legal disclaimers that apply to the journal pertain.

maintaining multiple homeostatic mechanisms allows it to exert several unrelated, beneficial effects including vaso-relaxation, [4] neurotransmission, [5] and immune functions. [6] Therefore it is not surprising that a variety of disease states including inflammation, erectile dysfunction, and multiple central nervous system disorders are associated with decreased *in vivo* NO production. [7] Of particular interest is the role of insufficient endogenous NO concentrations in the establishment and progression of atherosclerosis, the leading cause of cardiovascular disease worldwide. [8] The onset of atherosclerosis is commonly accompanied by increased levels of circulating low-density lipoproteins (LDL), which culminates in the adhesion of cholesterol to the inner blood vessel, composed of NO producing vascular endothelial cells. Essentially smothered and isolated from blood nutrients, these cells eventually undergo necrosis, and cease NO production. Lower physiological NO concentrations have been attributed to excessive SMC proliferation. [9]

The administration of NO-donors has been used to provide an exogenous source of NO, and lessen the deleterious effects associated with reduced endogenous NO production. Several NO donors including C, N, and S-nitroso, metal/NO complexes, and diazeniumdiolates have been reported. However, these compounds release NO rapidly in a single burst. [10, 11] Supplementation with such exogenous NO donors and/or overproduction of endogenous NO are known to confer harmful biological consequences. At elevated concentrations, interactions between reactive oxygen species (e.g. superoxide anion) and excess NO lead to the formation of peroxynitrates – compounds capable of exerting a wide variety of toxic effects. [12] Furthermore, the prolonged use of glyceryl trinitrate, a clinically approved NO donor, is known to induce nitrate tolerance. [13] Polymeric NO donors, capable of preventing rapid NO release have been reported as coating materials for implantable devices. [14–16]

To circumvent these deleterious effects associated with rapid NO release, compounds exhibiting a predictably slow and sustained release of NO are necessary. We have recently reported the preparation and characterization of both a low molecular weight (LMW) and a polymeric class of N-nitrosated secondary amines (NO donors), [7] each expressing the desirable attributes alluded to above. [17] Most importantly, both newly developed classes exhibited NO release in three distinct phases: a brief, fast releasing preliminary phase, an extended, more moderate second phase, and a slow and sustained final phase. We need to point out the possible concerns regarding the use of N-nitroso compounds as NO-donors. The amine nitrogen attached methyl group is a suspected alkylating agent for DNA modifications. For example, N-nitroso-Nmethyl-N-alkyl amines have been reported to induce bladder tumors in rats and hamsters. [18a] The fact that N-nitroso-N-ethylaniline is not carcinogenic lends further support to these hypotheses. [18b] Extensive discussions regarding the structural effects of nitrosamines and related compounds on their carcinogenicity can be found elsewhere. [18c] The concentrations of the non-methylated N-nitroso compounds reported in this study were effective at extremely low levels, at or below the micro-molar range.

The polymeric NO donors were prepared from the corresponding secondary amines – initially synthesized by the aromatic nucleophilic substitution of aliphatic diamines with 1,5-difluoro-2,6-dinitrobenzene (DFDNB). These polymers, along with select LMW compounds, exhibited excellent solvent resistance due both to inter- and intra- chain hydrogen bonding between the secondary amine moiety and the aromatic nitro groups. Polymers were insoluble in common organic solvents, dissolving only in aqueous concentrated sulfuric acid. [19] While highly desirable for some applications, nitrosation of these polymers could only be carried out at low temperatures in highly corrosive, aqueous concentrated sulfuric acid. A reduction in inter- and intramolecular hydrogen bonding would

allow for the facile nitrosation of both the polymeric and LMW secondary amines soluble in common organic solvents (including tetrahydrofuran) at room temperature.

Reported herein are the detailed preparation, isolation, and characterization of two isomeric families of LMW secondary amines, and their subsequent nitrosation to yield the corresponding NO-donors. The 20-day NO release rate profile and extended half-life of each new donor were determined in a phosphate buffered aqueous environment. In addition, because reduced glutathione (GSH) is a known scavenger of intracellular NO, the altered release rate profiles of representative donors from each family in the presence of GSH are also reported.

Cultures of human aortic smooth muscle cells (HASMCs) were employed to perform multiple cellular assays, to determine and reinforce the effects of each donor and its metabolites on vascular SMC proliferation and viability. After NO is released, the N-nitrosated compounds revert back to the corresponding secondary amine. Therefore, to accurately gauge the inhibitory effects of each NO-donor, it was crucial to determine any alteration of HASMC proliferation and/or viability attributable to these amine byproducts.

As discussed above, both NOS and arginase compete for the same substrate pool of L-arginine. In an effort to maximize intracellular NO concentrations without causing cell death, the potent arginase I inhibitor ABH was also tested in HASMC cultures. Inhibition of SMC arginase I can effectively enhance NO biosynthesis by increasing available concentrations of L-arginine to NOS. [20] Coupling this endogenous NO synthesis with the exogenous supply from the reported NO-donors is likely to further decrease HASMC proliferation, possibly in a synergistic manner. The anti-proliferative potential of each donor family, both independently and in combination with ABH were determined. In addition to cellular proliferation and viability assays, intracellular nitric oxide concentrations were monitored using a third cellular assay – which utilized the cell membrane permeable 4-amino-5-methylamino-2',7'-difluorescein diacetate (DAF-FM DA). The diacetate ester linkage is cleaved by intracellular esterase to form 4-amino-5-methylamino-2',7'-difluorescein (DAF-FM), which detects NO following two major pathways. The first involves its reactions with dinitrogen trioxide (produced from the intra-cell membrane reactions of NO with molecular oxygen) to form the triazole derivative (fluorescent signal). In the second pathway, the reaction of DAF-FM with reactive oxygen species (ROS) forms a DAF-FM radical which then reacts with NO to form the fluorescent triazole-containing compound. [21]

The chosen NO-donor, at its most efficient concentration, was combined with effective concentrations of ABH to achieve an optimal inhibition of HASMC proliferation. We report findings from these studies below.

2. Experimental

2.1 Chemicals & Equipment

The difluoride 2,4-difluoronitrobenzene (2,4-DFNB) (Aldrich) was distilled at reduced pressure, while 2,6-difluoronitrobenzene (2,6-DFNB) (Aldrich) was used as received. N,N-Dimethylacetamide (DMAC) and N-methylpyrrolidinone (NMP) (Aldrich) were dried over calcium hydride and distilled at reduced pressure. Toluene was distilled over calcium hydride. The diamines (Aldrich), with six to nine methylene units, were either purified by recrystallization using low boiling ligroin (b. p. 35 °C-50 °C) for solids or by distillation at reduced pressure for liquids. All other reagents for NO-donor synthesis were used as received. Griess Reagent was purchased from Oxford Biomed, Alexis, or Enzo Life Sciences. GSH was purchased from Aldrich. MTT (3-(4,5-dimethylthiazole-2-yl)-2,5-

diphenyltetrazolium bromide) assay kit, and cellular dimethyl sulfoxide (cDMSO) were purchased from ATCC. Live/Dead™ Viability/Cytotoxicity kit, DAF-FM and DAF-FM DA were purchased from Invitrogen Corporation. 2-(4-Carboxyphenyl)-4,4,5,5-tetramethylimidazole-1-oxyl-3-oxide, potassium salt (C-PTIO) was purchased from Aldrich. ABH, ultra pure lipopolysaccharide (LPS), interferon gamma (IFN- γ) were supplied by Enzo Life Sciences, Fisher, and PeproTech, respectively.

IR spectra were recorded on a Nicolet DxB FT-IR spectrophotometer using a thin film of the material on sodium chloride plate. Mass spectra of the secondary amines were obtained on a Hewlett-Packard Model 5995A Gas Chromatograph/Mass spectrometer with an ionization potential of 70 electron volts. Both H-1 and C-13 NMR spectra of the compounds dissolved in deuterated trichloromethane (CDCl₃) were recorded using a Varian Mercury 300 MHz or a Varian Inova 500 MHz instrument. Tetramethylsilane (TMS) was used as the internal standard for these measurements.

2.2 General Procedure for Secondary Amine Preparation (A6–A10 and B6–B10)

The preparation of compound **A7** is provided as a representative synthesis procedure of these compounds.

Heptylamine (1.3186 g, 0.0114 mole) and 2,4-DFNB, (0.9262 g, 0.0058 mole) were weighed into separate vials. Potassium carbonate (3.03 g, 0.022 mole, 50% excess) was transferred to a 100 mL three-necked round-bottomed flask fitted with a magnetic stir bar, nitrogen inlet, thermometer, and a Dean-Stark trap fitted with a condenser. Each glass vial used for weighing starting materials was rinsed with DMAC (5 mL) and the washings were transferred to the reaction vessel to ensure full transfer of any residual reagents. Next, an additional 4 mL of DMAC was added to the reaction vessel, followed by 15 mL of toluene. An initial exotherm of 5 °C was observed upon the dissolution of the starting materials, rendering the reaction mixture bright yellow in color. The reaction vessel was heated by an external temperature-controlled oil bath (with mild stirring) for 17 h at 125 °C. At the completion of the reaction, the vessel was cooled, the reaction mixture was diluted with dichloromethane, and then filtered through celite to remove all salts. The filtrate was evaporated at reduced pressure to yield a crude product that was subsequently dissolved in dichloromethane and washed with water. The organic layer was dried over anhydrous magnesium sulfate and filtered. The filtrate was evaporated at reduced pressure, and the resulting solid was further purified via recrystallization in absolute ethanol to yield yellow needles. Spectroscopic data for the secondary amines are supplied as supplementary information.

2.3 Nitrosation of Secondary Amines and Determination of the Extent of Nitrosation

Compound **B7** (0.0862 g, 0.00024 mole) was weighed in a 25 mL round-bottomed flask, fitted with a stopper. Tetrahydrofuran (THF) and glacial acetic acid (1:1 v/v) were added to dissolve the compound. The reaction vessel was then submerged in a cold-water bath prior to adding sodium nitrite in excess of greater than or equal to eight moles (0.1361 g, 0.0019 mole). When gaseous compounds were no longer visibly escaping the vessel, the water bath was removed and the temperature of the reaction mixture was allowed to rise to room temperature, and the vessel was stoppered. The reaction was allowed to continue at this temperature for 5–8 h for the **A** series of compounds and 24–48 h for **B** series. The progress of the reaction was monitored by IR spectroscopy. In both cases (isomeric families **A** and **B**), the time required to achieve 100 % nitrosation increased with length of the carbon chain substituents. Upon completion, the reaction mixture was transferred to a 100 mL Erlenmeyer flask containing an ice-cold saturated aqueous sodium chloride solution. The mixture was neutralized next with saturated aqueous sodium bicarbonate solution. Water was decanted

and the solid product was dissolved in dichloromethane. The solution was transferred to a separatory funnel and washed twice with ice-cold saturated aqueous sodium chloride solution and finally with ice water. The organic layer was then transferred to a beaker submerged in ice, and anhydrous magnesium sulfate was added. The solution was then filtered by gravity filtration into a round-bottomed flask and the solvent was removed at reduced pressure using a rotary evaporator. The nitrosated product, **B7'** was transferred and stored in a sealed container at 0 °C.

The extent of nitrosation was determined using IR spectroscopy. The decrease in the absorbance due to the secondary amino groups (3340 cm^{-1}) relative to the absorbance due to the aromatic double bond (1655 cm^{-1}) was measured before and after nitrosation to obtain the extent of nitrosation for each sample (Tab. 1).

2.4 NO Release Rate Determination

2.4.1 Griess Reagent Test—The detailed procedure has been provided elsewhere. [17] Briefly, nitrosated compounds (**A6'**–**10'**) and (**B6'**–**10'**), were weighed into separate 25 mL round bottom flasks wrapped in aluminum foil, and equipped with a magnetic stir bar and cadmium pellet (~1 mg) previously washed with 0.1 M HCl and 0.1 M NH₄OH solutions. At $t=0$, a volume of 1X PBS was added to create a 0.0125 M solution (0.0250 M NO). Aliquots were withdrawn over the course of the reaction to monitor NO release, from $t=0$ to $t=12$ h every one hour, from $t=12$ h to $t=24$ h, every four hours, and from $t=24$ h to 48 h, every eight hours. After 48 h, aliquots were removed in 24 h increments.

Aliquots (200 μL) were transferred to a 1.5 mL plastic microtube (Fisher), and centrifuged at 2000 rpm for 2 minutes. Next, three 50 μL aliquots of the supernatant were transferred to separate wells of a 96 well plate and combined with 50 μL of 1X PBS and 100 μL of Griess Reagent. After a five-minute incubation period at room temperature, the absorbance of each well was determined at 550 nm using a micro plate reader (Molecular Devices) and SoftMax Pro software. The NO release rate was determined by plotting the absorbance vs. time. The same procedure was followed to determine the NO-release profiles of **A6'**, **A9'**, **B8'**, and **B10'** in 1X PBS solution containing reduced glutathione (GSH, 5 mM). Since GSH does not react with Griess Reagent, a new calibration curve (with GSH) was not necessary for these measurements.

2.4.2 DAF-FM—Approximately 100 mg of each of the nitrosated material, **A7'**, **B7'**, **A10'** (with GSH), and **A10'** (without GSH) was added to a 25 mL round bottomed flask, and diluted with 1X PBS solution. The flask was fitted with a magnetic stir bar and a stopper, wrapped in aluminum foil, and placed over a stir plate at a moderate speed for the duration of the reaction. At the same designated time intervals (Section 2.4.1), 200 μL aliquots were transferred to a 1.5 mL Eppendorf micro tube and centrifuged for 2 minutes at 200 rpm. Three 50 μL aliquots of the resulting supernatant were added to designated wells of a fluorescence grade 96 well plate (Corning) and further diluted with an additional 50 μL of fresh 1X PBS, for a total volume of 100 μL /well. Finally, 1.0 μL of 1.0 mM DAF-FM/cDMSO working solution was added, yielding a final DAF-FM concentration of 10 μM per well. The plate was covered and incubated at 37 °C for 30 minutes. Fluorescence excitation and emission maxima were recorded at 495 and 515 nm respectively using and Molecular Devices micro plate reader and SoftMax Pro software.

2.5 Verification of Release of NO from **A6'** using C-PTIO

2.5.1 Analysis in 1X PBS Solution—Three 50 mL, one necked, round-bottomed flasks (labeled 1, 2, and 3) were equipped with a magnetic stir bar and previously washed cadmium pellets as described above (Section 2.4.1). Next, precisely 50 mg (± 0.1 mg) of **A6'** were

added to flasks 1 and 2. A 1.3 mg sample of the solid probe was dissolved in 1X PBS to render a 100 μM C-PTIO solution. A 20 mL aliquot of the freshly prepared solution was then delivered to flasks 1 and 3 using a volumetric pipette. Flask 2 received an equal volume of pure 1X PBS. All three flasks were capped and gently stirred at room temperature for 5 days. At 24 h increments, 500 μL aliquots were transferred to individual micro-centrifuge tubes, and spun at 13,000 rpm for 2 minutes. Aliquots (100 μL) of each supernatant were transferred to separate wells of a 96-well plate and gently mixed with an equal volume of Griess Reagent. The absorbance of each well was then measured at 550 nm with microplate reader. Triplicate wells were prepared for each sample, with the average absorbance being plotted as a function of time.

2.5.2 Analysis in Supplemented Smooth Muscle Cell Medium—Three round-bottomed flasks were fitted and solutions analyzed using the same methods outline in Section 2.5.1 above with the following modifications: Complete SMC Medium (2% Fetal Bovine Serum (FBS), 1% Growth Serum, 1% Penicillin) was used in place of 1X PBS. The NO-donor (**A6'**) was added as a 2 mM solution in cDMSO (200 μL , final concentration 20 μM). Centrifugation prior to addition to 96-well plate was omitted. Except for absorbance measurements, [24a] all other procedures were performed in a sterile environment.

2.6 Cellular Studies

2.6.1 Human Aortic Smooth Muscle Cell Culture—Cultures of human aortic smooth muscle cells (HASMCs) were developed and maintained in accordance with the procedural guidelines recommended by both ScienCell and ATCC. To ensure adequate attachment, the 75 cm^2 culture flasks (Corning) required a specially treated CellBIND® surface. Cells were grown in SMC specialty medium (5% FBS, 1% Growth Serum, 1% Penicillin, (ScienCell)) to 95% confluency before passage with trypsin. Following passage six, cells were quantified (cells/mL) using a hemacytometer, further diluted to a concentration of 30,000 – 35,000 cells/mL using SMC medium, then transferred as 100 μL aliquots to clear, colorless, 96 well plates (Corning, with CellBIND surface) to provide 3000 to 3500 cells per well (cpw). The seeded plates were incubated at 37 °C for 16–24 h to ensure stable cellular attachment. The cellular population was synchronized to G₀ by removing the complete medium from each well and replacing it with serum-free SMC medium (100 μL). The plates were again incubated at 37 °C for 24–48 h prior to subsequent testing.

2.6.2 HASMC Exposure to Secondary Amines—Solutions of each secondary amine (**A6–B10**) were prepared in cellular DMSO (cDMSO) at five concentrations (10, 100, 500 μM , 1.0 and 2.0 mM). An aliquot of each amine solution was combined with complete SMC medium to render a 1% cDMSO/medium solution (v/v) (0.1, 1, 5, 10 and 20 μM), to be added to SMC cultures, in addition to positive (medium only) and negative (medium and 1% DMSO) controls. The serum-free medium was replaced with 100 μL of each sample medium solution (2% FBS, 1% Growth Serum, 1% Penicillin), and plates were incubated for 48 h, followed by the addition of 100 μL of fresh medium to each well for a final volume (200 μL). Plates were again incubated for 48 h, before MTT or LIVE/DEAD analyses. The final testing concentration of cells after 96 h was 48,000–56,000 cpw.

2.6.3 HASMC Exposure to NO-Donors—Solutions of each nitrosated compounds (**A6'–A10'** and **B6'–B10'**) were prepared in cDMSO at the same five concentrations as used with the secondary amines. Each sample was combined with complete SMC medium to yield a 1% cDMSO/NO-donor solution (v/v) (0.1, 1, 5, 10 and 20 μM). After the removal of the serum free medium, each solution was added to the predetermined wells in a manner identical to that outlined in Section 2.6.2. Following exposure, MTT, LIVE/DEAD, and DAF-FM DA analyses were performed.

2.6.4 HASMC Exposure to ABH—Prior to the addition of ABH, LPS (50 $\mu\text{g}/\text{mL}$) and INF- γ (50 ng/mL) were added, and well plates were incubated at 37 $^{\circ}\text{C}$ for six hours. LPS and the cytokine were removed, and replaced with ABH/SMC medium (100 μL) solution at varying concentrations (1, 10, 100 μM , 1.0 and 5.0 mM). Similar protocols (outlined in Section 2.6.2) were followed for the incremental additions of ABH solution to the cells.

2.6.5 Synergistic Addition of ABH and NO-donors—To induce iNOS, cells were first incubated with LPS (50 $\mu\text{g}/\text{mL}$) and INF- γ (50 ng/mL) in SMC medium for six hours at 37 $^{\circ}\text{C}$. Cytokines were then removed, and ABH (100 μL , 5 mM) and varying concentrations of each NO-Donor (Tab. 2) in SMC medium were added to each well, and cells were again incubated at 37 $^{\circ}\text{C}$ for 48 h. A second aliquot of 100 μL SMC medium solution (100 μL) containing the specified ABH/NO-donor combination was added, followed by a final 48 h incubation period at 37 $^{\circ}\text{C}$ before undergoing subsequent viability and NO determination assays.

2.6.6 MTT Proliferation Assay—At the end of the incubation period, 10 μL MTT reagent was added to each well. Plates were incubated at 37 $^{\circ}\text{C}$ for four to six hours. Finally, MTT detergent (100 μL) (ATCC) was added to each well. Plates were incubated at room temperature, in the absence of light for a minimum of two hours (24 h maximum) yielding a homogeneous purple solution in each well. The absorbance of each well was measured using a plate reader at 570 nm. Comparisons between treatment groups were made by t-test using the Minitab software program. A value of $p > 0.05$ was considered statistically equal.

2.6.7 LIVE/DEAD Assay—Optimum reagent concentrations for HASMCs, found in accordance with the Invitrogen protocol, were determined to be 0.50 μM and 0.25 μM for Ethidium Homodimer-1 (Eth-1) and Calcein AM (CAM), respectively.

Corning black, polystyrene 96 well microplates, with clear bottom and CellBIND surface were prepared in the same manner as the clear microplates mentioned above, and underwent identical treatments with compound solutions for toxicity determination. Because dead HASMCs become unattached, the medium containing the dead cells was removed from each well, and transferred to individual 0.5 mL micro-centrifuge tubes. Adherent cells were washed twice with PBS (100 μL) solution to remove residual medium.

The tubes containing the dead cells were centrifuged at 2500 rpm for 3 min. The medium was removed, and the pellet of dead cells was washed in PBS solution (250 μL) and centrifuged. The supernatant was removed, and the cells were again suspended in fresh PBS solution (100 μL), and then returned to the original well (with adherent cells). A PBS solution (100 μL) of Eth-1 (0.5 μM) and CAM (0.25 μM) were added to each well. Plates were incubated at room temperature for 45 min. The percentages of both live and dead cells were determined using a fluorescent plate reader (Molecular Devices) at ex/em 495/530 nm (CAM) and 528/645 nm (Eth-1) respectively.

2.6.8 Intracellular NO Determination using DAF-FM DA—Corning black, polystyrene 96 well microplates, with CellBIND surface were prepared as described in Section 2.5.1 and then treated with the predetermined compound solutions (NO-donors, ABH, or a combination of ABH and NO-donor). After exposure, a DAF-FM DA (10 μM) solution in PBS (100 μM) was added to each well. Plates were incubated at room temperature in total darkness for 60 min. The DAF-FM DA solution was then removed, and cells were washed (3X) with PBS to remove excess probe. Fresh medium (or PBS) was added, and plates were again incubated under the same conditions to allow for complete de-esterification of DAF-FM DA. Fluorescence was then recorded at ex/em 495 nm and 515 nm, respectively.

3. Results and Discussion

3.1 Preparation of Secondary Amines A6-A10 and B6-B10 from Aliphatic Homologous Monoamines and 2,4-/2,6-DFNB

Secondary amines were prepared from homologous aliphatic primary amines, containing six to ten carbon atoms, and 2,4 or 2,6-dinitrofluorobenzenes (2,4-DFNB or 2,6-DFNB) (Scheme 1). All reactions were carried out at 120 °C for ~24 h. Under these reaction conditions, the desired compounds could be prepared in high yields (Supplementary Information). Thin layer chromatography (TLC) coupled with GC/MS analyses of the reaction mixtures indicated the absence of side products. This scenario changed rapidly when any one of these reactions was conducted above 130 °C. At these temperatures, in addition to the desired product, the formation of numerous other compounds (derived from one major intermediate) was observed. These findings suggest that attempts to form high molecular weight polymers using diamines at elevated temperatures (necessary for the reactions to proceed to completion in an increasingly more viscous medium and with decreasing concentrations of reactive ends) would be unsuccessful. Details of these side reactions will be reported separately.

3.2 Nitrosation of Secondary Amines A6-A10, B6-B10 and Extent of Nitrosation Determination

Nitrosation of compounds **A6–A10** and **B6–B10** performed in glacial acetic acid/THF (1:1 v/v) in the presence of excess sodium nitrite (Scheme 1) could be achieved quantitatively (Table 1). The rate of nitrosation for the **B** (2,6-) family of isomeric diamines was substantially slower than the corresponding **A** (2,4-) isomers due to the closer proximity of the nitro group to both amine groups compared to that of the corresponding 2,4-substituted compounds. This phenomenon is typical when NO acts as the nitrosating agent of weakly basic, N-alkyl aryl secondary amines. [22] In addition, both families exhibit a decrease in the rate of nitrosation due to steric interferences with increasing aliphatic chain lengths. For example, the conversion time of **B6** to **B6'** was approximately 24 h, in contrast to 48 h required for complete nitrosation of **B10**.

3.3 NO Release Rate Determination

The amount of NO released from each nitrosated compound (**A6'–A10'** and **B6'–B10'**) was measured using Griess Reagent [17] over a period of 20 days (Fig. 2a and 2b). From an examination of these figures, two trends are clearly discernible. First, the rate of NO release increases as the number of methylene units increases. Second, the release of NO occurs in three distinct stages; an initial fast phase (~0–10 h), a moderately fast phase (~10–200 h) and a very slow and sustained phase (~200–480 h) respectively. These observations are consistent with previously reported data based on nitrosated model compounds prepared from DFDNB. [17] The calculated apparent half-lives ranged from 60 h to 105 h for **A6'–A10'** and from 62 h-140 h for **B6'–B10'** (Table 1), which are significantly longer than many currently available commercial NO donors. [10,23] The NO release profiles of compounds **A7'** and **B7'** were also determined using DAF-FM, a NO and /or N₂O₃ probe (Fig. 2c). An analysis of Fig. 2c indicates that irrespective of the NO-probe used (Griess reagent (Fig. 2a and 2b) or DAF-FM), both the release profiles and the rates (**A7'** and **B7'**) remain unchanged. A control experiment with a solution of DAF-FM in PBS did not exhibit an enhanced fluorescent signal.

A comparison of half-lives between any two isomeric NO donors (e.g. **A8'** and **B8'**) indicates that the 2,6-isomer exhibits a higher half-life compared to the corresponding 2,4-isomer. This phenomenon possibly due to the loss of the radical species NO, results in the formation of electron deficient nitrogen radical in closer proximity to the electron

withdrawing nitro group (energetically less favorable) than that formed from the corresponding 2,4-isomers. In addition, the differing steric environments of the N-NO moieties in these two families may further contribute to the differing NO release rates.

In order to ascertain the nature of the NO species being released from the N-aryl-N-alkyl-N-nitrosamines, **A6'**–**A10'** and **B6'**–**B10'**, C-PTIO and Griess reagent were employed (Section 2.4.1). [24] C-PTIO is also known to interact with peroxyxynitrite anion *in vivo* where superoxide radical anions are present. [25] In the present instance our experiments were carried out in solvent systems of PBS solution or using the SMC culture medium. Under these conditions, superoxide radical anions are not formed, which excludes the formation of peroxyxynitrite anion and the resulting interference during the C-PTIO tests. Data from these studies in PBS solution and in a solution of supplemented culture medium are displayed in Fig. 3a and Fig. 3b respectively. From an examination of these figures one observes the significant increase in nitrite concentration in the presence of C-PTIO than in its absence, which is indicative of the rapid capture of the NO radical species (and its subsequent conversion to nitrite anion) [25a] released from the NO-donor, **A6'**. The formation of NO from the NO-donors under consideration is not unexpected in view of the earlier findings. [26] It has been shown that N-aryl-N-alkyl-N-nitrosamines with linear alkyl groups and electron withdrawing nitro substituent in the ortho or para position to the nitrogen atoms of the amine moieties, structural features similar to the NO-donors under consideration, undergo homolytic cleavage to form NO. The ease of homolytic cleavage was attributed to the delocalization of electron density on the nitrogen atoms of the amine groups and consequent weakening of the N-NO bond due to the loss of double bond characteristics. [26] Additional theoretical calculations and experimental studies have been reported in support of the favorable formation of NO radical species over that of nitrosonium ion (from heterolytic cleavage), with increasing delocalization of the lone pair on the nitrogen atom of the amine nitrogen atom. [27]

The subsequent reactions of nitric oxide and oxygen in an aqueous environment produce mono and dinitrogen species including nitrite, nitrate, dinitrogen trioxide and dinitrogen tetroxide. Dinitrogen oxides may undergo further decompositions to produce nitrites and nitrates. [28] Nitrites and nitrates undergo intracellular reduction to nitric oxide by mitochondrial aldehyde dehydrogenase. [29]

Additionally, we have investigated if and how the NO-release profiles may be affected under aerobic conditions in the presence of intracellular glutathione (GSH). [30] The concentration of GSH was maintained at 5 mM [31] in PBS solution and the NO-release profiles of four NO donors, **A6'**, **A9'**, and **B8'**, **B10'**, determined over a period of 20 days, are displayed in Fig. 4a and 4b respectively. When compared with Fig. 2a and 2b, the NO release rate patterns in the presence of GSH are similar; NO is still released in three distinct stages and the NO release rate still increases with the number of methylene units. However, important differences exhibited by all four compounds tested are apparent. Of considerable importance is the overall decrease in the amount of NO released to approximately one third of that observed in the absence of GSH. Furthermore, the initial “fast” phase and second moderately fast phase are considerably shorter in the presence of GSH.

S-nitrosothiols (RSNO), including nitrosated glutathione (GSNO), act as NO storage and transport vehicles *in vivo*. GSH is known to react with NO, either produced endogenously or released from an exogenous source(s). It has been previously reported that the addition of a catalytic amount of copper (I) induces NO release from GSNO. [32] We have confirmed these earlier findings with the addition of a catalytic amount (< 0.5 mg) of solid cuprous chloride to the reaction mixture containing **B10'** with GSH. One hour after the addition of copper, it was observed that the total amount of NO released into solution was equal to that

determined for **B10'** in the absence of GSH (Fig. 4b). These observations clearly suggest that the presence of GSH does not affect the NO-donor's ability to release NO. Similar results were obtained when a different probe, DAF-FM was used to monitor the release rate profile for **A10'** with and without GSH (Fig. 4c). [33] A lack of increased fluorescent signal from a mixture of GSH and DAF-MF in PBS solution confirmed that the trends observed in the fluorescent intensities (Fig. 4c) are due to NO or related species.

The secondary amines were nitrosated using sodium nitrite (Section 2.2), in an acidic medium. Griess reagent detects NO indirectly, by determining the total nitrite (formed from NO) concentration. [17] To ensure the NO concentrations determined using Griess reagent were solely due to NO released from the NO-donors, rather than from any residual nitrite from the reaction mixture, a control experiment was undertaken. A PBS solution of sodium nitrite (0.0125 M) was treated with Griess reagent. The nitrite concentration measured over 20 days remained constant (Fig. 2a), unlike the three-stage release of NO from the NO-donors. These observations clearly confirm that the measured concentrations of NO derived nitrite are solely due to the NO-donors.

3.4 Cell Culture Studies

3.4.1 Secondary Amine Toxicity—After the release of NO, the N-nitroso compounds revert to the corresponding secondary amine precursors, which remain exposed to cells in the culture medium. Therefore, it was imperative to examine the potential influences **A6–A10** and **B6–B10** may exert towards HASMCs. An MTT assay was performed to identify whether the secondary amines exert any anti-proliferative or toxic effects on HASMCs. Because the amines were sparingly soluble in aqueous medium, a combination of cDMSO and SMC Cellular Medium (DMSO/medium, 1% v/v) was used as the vehicle. Data obtained from MTT studies are shown in Figs. 5a (**A6–A10**) and 5b (**B6–B10**) respectively. For clarity, data from 0.1 and 1 μM amine concentrations are not shown in the figures, however the complete data set is displayed in Table S.B1, Appendix B (Supplementary Material). An examination of these figures first illustrates that 1% DMSO ((-) control) results in a decrease in the number of viable cells when compared to SMC medium alone ((+) control). [34] Secondly, all of the amines tested, with the exception of **B9** and **B10**, exhibited equal or less toxicity than the vehicle at four or more concentrations, suggesting any decrease in cell viability is a consequence of the vehicle's presence. For example, compound **A8** exhibited higher toxicity at a lower concentration (0.1 μM); however at higher concentrations (1, 5 and 20.0 μM), it was found to be equally or less toxic than the vehicle. These variations can be attributed to experimental artifacts. Conversely, the presence of **B9** and **B10** at the three highest, and all tested concentrations respectively, induces a statistically significant decrease in cell viability compared to the vehicle alone.

In order to further confirm the trends observed in the MTT assay, a LIVE/DEAD assay was performed to ascertain whether the secondary amines were decreasing cell proliferation rates or inducing cell death. Results from these studies are displayed in Fig. 6a (**A6–A10**) and 6b (**B6–B10**). Consistent with the MTT assay, treatment with cDMSO alone (the vehicle) results in a statistically significant decrease (~12%) in the number of live cells. Additionally, the concurrent increase in the number of dead cells (Fig. 6a and 6b) indicates that the presence of the vehicle results in cell death in contrast to inhibition of proliferation. Furthermore, each secondary amine, except **B9**, and **B10**, showed a statistically equal percentage of live and dead cells as the vehicle. This suggests that the vehicle, rather than the secondary amine (barring the above exceptions) is responsible for the decrease in cell viability. Compounds **B9** and **B10**, on the other hand, caused a statistically significant decrease in the number of live cells, while maintaining statistically equal numbers of dead cells as the vehicle. These observations indicate that both **B9** and **B10** exert anti-

proliferative effects rather than causing cell death. Collectively the amines tested do not cause cell death irrespective of the concentrations used in these experiments. Details of the performed statistical analyses (p values and t-stat values) are supplied as supplementary data in Appendix C.

3.4.2 Effects of Exogenous NO-Donors (A6'–B10') on HASMC Proliferation—

The addition of our NO-donors (A6'–A10' and B6'–B8') at various concentrations (Section 2.6.3) to cultures of HASMCs was performed to determine the most effective concentrations required to obtain maximum proliferation inhibition, without initiating cell death (e.g. necrosis or apoptosis). The results obtained from the MTT, LIVE/DEAD, and DAF-FM DA assays are displayed in Fig. 7, 8, and 9 respectively. In Fig. 7, for the purpose of clarity, data from 0.1 and 1 μM N-nitrosated amine concentrations are not shown, however the complete data set is shown in Appendix B, Table S.B2 (Supplementary Material). An examination of both the MTT assay and LIVE portion of the LIVE/DEAD test results, Fig. 7, 8a and 8c respectively, indicates that all of the NO-donors confer anti-proliferative effects on HASMCs at concentrations less than or equal to 20 μM . Furthermore, for all of the compounds tested in both isomeric families (excluding B7'), the extent of proliferation inhibition is enhanced with increasing concentrations of NO-donors. In contrast, B7' hindered proliferation more effectively with increasing concentrations from 0.1 μM to 5 μM , however, further increases in the concentrations had less salutary effects.

Of equal importance are the DEAD test results (Fig. 8b and 8d). As mentioned in Section 3.4.1, the presence of cDMSO initiates death in a small, yet significant percentage of cells. However, with the addition of a given NO donor, the amount of dead cells remains statistically constant, attributable to the presence of the vehicle. These observations indicate the presence of the NO-donors is responsible for a statistically significant decrease in viable (LIVE) cells by influencing a decrease in cell proliferation rather than initiating cell death. It should be pointed out that under mild NO induced oxidative stress, SMCs undergo apoptosis rather than a termination in cell proliferation. [35,36] LIVE/DEAD assays conducted by us indicate a lack of cell death when NO-donors are administered, which has led us to attribute the decrease in viable cell population to the inhibition of proliferation. Furthermore, the maximum concentration of NO delivered from the highest dose of a NO-donor (20 μM) to 48,000–56,000 SMCs did not exceed 40 μM (0.7–0.8 nM/cell). These calculations are based on the hypothesis that a NO-donor loses both the NO moieties over a 96 h period and all NO or NO derived species enter the cells. The calculated intracellular concentration of NO is significantly less than 130 ± 10 nM, which a single smooth muscle cell can withstand without induction of oxidative stress. [37] These observations coupled with the data from LIVE/DEAD assays establish the decrease in viable cells to the inhibition of proliferation only.

Finally, the addition of NO-donors to HASMC culture should increase the overall presence of NO within the cells being treated. DAF-FM DA was used to access the inner cellular environment, and assess the intracellular NO and/or N_2O_3 concentration. [21] The results of the DAF-FM DA assays for both families of compounds are illustrated in Fig. 9a (2,4-isomers) and 9b (2,6-isomer). An examination of these figures demonstrates an increase in intracellular NO (increasing fluorescence signal) with increasing NO-donor concentrations with the exception of B7'. Irrespective of the various transformation reactions the released NO may have undergone, these findings reiterate the fact that NO is being released, and the concentration available for cellular use is determined by the initial concentration of the NO-donor used in these experiments. In the case of B7', the backbone of each side chain consists of an even number of sp^3 hybridized atoms (a nitrogen and seven carbon atoms). In contrast, B6' and B8', are each flanked by two chains composed of an odd number of atoms. We speculate that these attributes dictate the solubilities of these three compounds in cDMSO. It

is not unlikely that **B7'** (side chains with an even number of atoms) can achieve a greater degree of packing resulting in decreased solubility compared to **B6'** and **B8'**. At concentrations $5 \mu\text{M}$, **B7'** exhibited the expected pattern of proliferation inhibition. However, when the concentrations of **B7'** were increased to 10 and 20 μM , the average absorbances decreased, due possibly to the precipitation of **B7'** (Fig. 9b). On the other hand, **B6'** and **B8'** being devoid of this solubility issue release increasing amounts of NO with increasing concentrations. These effects due to the solubility differences are also observed with MTT (Fig. 7b) and LIVE/DEAD (Fig 8c) assays.

3.4.3 Effects of ABH Induced, Endogenous NO Increase on HASMC

Proliferation—The introduction of ABH, the most potent inhibitor of arginase, [20] should increase the bioavailability of L-arginine to NOS thereby enhancing endogenous NO production. In order to verify this established hypothesis, PBS solutions of ABH were added in various concentrations to HASMC culture (Section 2.6.4). Solutions of LPS and the cytokine IFN- γ were added to the culture medium to activate inducible NOS (iNOS) 6 h prior to ABH administration. [38] The cells were subsequently analyzed by both MTT and LIVE/DEAD assays. Results from these studies are displayed in Fig. 10a and 10b respectively. Analyses of these figures indicate that the inhibition of HASMC proliferation increases with increasing concentrations of ABH. The highest concentration of ABH was maintained at 5 mM (48% inhibition), [39] which was more effective in inhibiting cell proliferation than the 1 mM ABH concentration (35%). ABH (5 mM) was used in combination with the selected NO-donor (at optimum concentrations) to identify any synergistic effects. Findings from these studies are delineated in Section 3.4.4 below.

DAF-FM DA was used again to determine the intracellular concentrations of NO and/or N_2O_3 . [21] The results from these experiments are displayed in Fig. 10c; the amount of intracellular NO rises with increasing concentrations of ABH. Control experiments using solutions of ABH, DAF-FM DA and ABH, DAF-FM in the supplemented culture medium failed to produce enhanced fluorescent signals. These findings clearly indicate that sufficient inhibition of arginase, and the consequent build-up of the L-arginine pool, allows for increased production of intracellular NO.

3.4.4 Synergistic Effects of NO-donors and ABH on HASMC Proliferations

—Of the eight NO-donors tested, compounds **A6'** and **B6'** (20 μM) were chosen for in tandem addition with ABH (5 mM) to investigate their combined effects on HASMC proliferation. To be considered synergistic, the reduction in proliferation rendered must be greater than the sum of reduction caused by each component individually. Results from both the MTT viability assay (Fig. 11a) and the LIVE/DEAD test (Fig. 11b) reveal that both NO-donors in the presence of ABH more effectively inhibit HASMC proliferation than any of the three compounds alone. Furthermore, Fig. 11b illustrates that the combined supplementation does not initiate additional cell death compared to the vehicle alone. To further support these observations, the amount of intracellular NO and/or N_2O_3 present, as detected by DAF-FM DA (Fig. 11c), [21] is greater in cells treated with the NO-donor or ABH than the untreated cells. Tandem supplementation with these two reagents results in a larger increase of intercellular NO (compared to the negative control) than the sum of singular NO-donor or ABH additions. Table 2 summarizes the comparison between the singular and in tandem additions. The data contained allows for the determination of synergistic, additive, or simply a more effective inhibition of HASMC proliferation. For example, **A6'** with ABH exhibited an additional 13% decrease (64%) in cell proliferation when compared to the sum of percent decreases (51%) from each of the components alone. On the other hand, the combination of **B6'** and ABH brought about an additional proliferation reduction of only 2% (48%, compared to 46%); less than the combined effects of **A6'** and ABH, which may be

attributable to the higher half-life of **B6'**. The anti-proliferative effects of two arginase inhibitors, S-(2-boronoethyl)-L-cysteine (BEC) and L-N^G-hydroxy-L-arginine (L-NOHA) have been reported. [40] The anti-proliferative effects of ABH are exerted in a similar manner by simultaneously increasing endogenous NO production and inhibiting polyamine formation. The latter is accomplished as ABH inhibits arginase I, down regulating the production of ornithine-the precursor to polyamines. Since polyamines are known to increase NO-independent HASMC proliferation, [40,41] a decrease in polyamine concentrations would result in a decrease in HASMC proliferation as well. Therefore, the co-administration of a NO-donor along with a potent arginase inhibitor is likely to be synergistic rather than additive.

The efficacy of the NO-donors (with and without ABH addition) used in this study is comparable to other NO-donors reported previously. [42] Our most effective NO-donors, **A6'** and **B6'** (20 μ M) confer ~20% inhibition of proliferation observed in cell culture studies performed over a 96 h period. These NO-donors exhibit relatively long apparent half-lives and release NO in a sustained manner. Thus the observed extent of inhibition of proliferation is likely to be smaller than one might expect to observe *in vivo* or in the presence of other NO-donors, which release NO rapidly in a single high concentration burst. Furthermore, tandem addition of NO-donors with ABH produces inhibition of proliferation comparable to conventional NO-donors present at higher, near toxic concentrations including, SNAP (30 μ M), DETA-NO (100 μ M) and NCX4016 (30 μ M). [42]

4. Conclusions

Collectively, the above results verify the successful synthesis of two different isomeric families of secondary amines via nucleophilic aromatic substitution reactions, from two activated aromatic difluorides. The resulting secondary amines were subsequently nitrosated, with 100% efficiency to prepare the desired NO-donors. Due to the strategic placement of the strong electron withdrawing nitro group in relation to the two N-NO moieties, each family of NO-donors were able to release NO in a distinct and controlled, three-phase manner. In the first phase, NO was released at the fastest rate. The second, moderately fast phase, which lasts from 10 to ~200 hours is followed by the continual, slow releasing third stage, which ensures a steady, physiologically safe source of NO to maintain the required NO concentrations.

These newly developed NO-donors exhibited a lack of toxicity toward HASMCs, and inhibited their proliferation. Introduction of the NO-donors in tandem with ABH increased both the exogenous and endogenously released, amount of intracellular NO. This decrease in HASMC proliferation was higher than the combined decrease due to the individual administrations of NO-donor or ABH. These synergistic effects may prove useful in the prevention of atherosclerosis and/or the formation of large, vessel clogging plaques.

Supplementary Material

Refer to Web version on PubMed Central for supplementary material.

Acknowledgments

The work was supported in part by Bridge to Commercialization Fund (CMU) and National Institute of Health (NIH) Award Number R15HL 106600 from the National Heart, Lung and Blood Institute (NHLB). The content is solely the responsibility of the authors and does not represent the official views of NHLB or NIH.

References

1. Ignarro, LJ. Nitric Oxide Biology and Pathobiology. Ignarro, LJ., editor. San Diego: Academic Press; 2000. p. 3-19.
2. Eroy-Reveles AA, Marschark PK. Future Medicinal Chemistry. 2009; 8:1497. [PubMed: 21426062]
3. Alderton WK, Cooper CE, Knowles RG. Biochem. J. 2001; 357:593. [PubMed: 11463332]
4. Ignarro LJ. Biochem. Pharmacol. 1991; 41:485. [PubMed: 1847633]
5. Zhou L, Zhu DY. Nitric Oxide. 2009; 20:223. [PubMed: 19298861]
6. Bogdan C. Nature Immunology. 2001; 2:907. [PubMed: 11577346]
7. Cai, TB.; Wang, PJ.; Holder, AA. Nitric Oxide Donors for Pharmaceutical and Biological Applications. Wang, PG.; Cai, TB.; Taniguchi, N., editors. Wiley-VCH; Weinheim: 2005. p. 3-31.p. 59-60.
8. McGill HC Jr, McMahan CA, Gidding SS. Circulation. 2008; 117:1216. [PubMed: 18316498]
9. Schwartz CJ, Valentine AJ, Sprague EA, Kelley JL, Nerem RM. Clin. Cardiol. 1991; 14:I-1. [PubMed: 2044253]
10. Napoli C, Ignarro LJ. Annu. Rev. Pharmacol. Toxicol. 2003; 43:97. [PubMed: 12540742]
11. Wang PG, Xian M, Tang X, Wu X, Zhong W, Tingwei C, Janczuk AJ. Chem. Rev. 2002; 102:1091. [PubMed: 11942788]
12. Davis LK, Martin E, Turko IV, Murland F. Annu. Rev. Pharmacol. Toxicol. 2001; 41:203. [PubMed: 11264456]
13. Munzel T, Daiber A, Mulsch A. Circulation Research. 2005; 97:618. [PubMed: 16195486]
14. Wan A, Gao Q, Li H. J. Mater. Sci. Mater. Med. 2009; 20:321. [PubMed: 18807152]
15. Xu H, Reynolds MM, Cook KE, Evans AS, Toscano JP. Organic Lett. 2008; 10:4593.
16. Wu Y, Meyerhoff ME. Talanta. 2008; 75:642. [PubMed: 18585126]
17. a) Wang J, Teng Y, Yu H, Oh-Lee J, Mohanty DK. Polymer J. 2009; 41:715.b) Teng Y, Kaminski GA, Zhang Z, Sharma A, Mohanty DK. Polymer. 2006; 47:4004.
18. a) Lijinsky W. Cancer and Metastasis Reviews. 1987:301. [PubMed: 3319273] b) Traul KA, Takayama K, Kachevsky V, Hink RJ, Wolff JS. J. Appl. Toxicol. 1981; 1(3):190. [PubMed: 7185884] c) Lijinski, W. Nitrosamines and Related N-Nitroso Compounds Chemistry and Biochemistry. In: Loepky, RN.; Michejda, CJ., editors. Am. Chem. Soc. Symposium Series American Chemical Society. Vol. 553. Washington D. C.: 1994. p. 250
19. Yu H, Payne T, Mohanty DK. Chem. Biol. Drug Des. 2011; 78:527. [PubMed: 21740530]
20. a) Kim NN, Cox D, Baggio RF, Emig FA, Mistry SK, Harper SL, Speicher DW, Morris SM, Ash DE, Traish A, Christianson DW. Biochemistry. 2001; 40:2678. [PubMed: 11258879] b) Cox DJ, Cama E, Colleluori, Pethe S, Boucher J, Mansuy D, Ash DE, Christianson DW. Biochemistry. 2001; 40:2689. [PubMed: 11258880] c) Costanzo LD, Sabo G, Mora A, Rodrigiez PC, Ochoa AC, Centeno F, Christianson DW. Proc. Nat. Acad. Sci. USA. 2005; 102:13058. [PubMed: 16141327]
21. a) Cortess-Krott M, Mateos-Rodriguez A, Kunhnl G, Brown G, Feelisch M, Kelm M. Free Rad. Biol. And Med. 2012; 53:2146. [PubMed: 23026413] b) Kojima H, Urano Y, Kikuchi K, Higuchi T, Hirata Y, Nagano T. Angew. Chem. Int. Ed. Engl. 1999; 38(21):3209. [PubMed: 10556905] c) Nakatsubo N, Kojima H, Kikuchi K, Nagoshi H, Hirata Y, Maeda D, Imai Y, Irimura T, Nagano T. FEBS Lett. 1998:263. [PubMed: 9607324]
22. Williams DLH. Adv. Phys. Org. Chem. 1983; 19:381.
23. [Date Accessed 1st August 2012] www.scbt.com/chemicals-table-nitric_oxide_donors.html.
24. a) Amano F, Noda T. FEBS Lett. 1995; 368:425. [PubMed: 7543422] b) Miura K, Yamanaka S, Ebara T, Okumura M, Imanishi M, Kim S, Nakatani T, Iwao H. Jpn. J. Pharmacol. 2000; 82:261. [PubMed: 10887957] c) Takahasi K, Numata N, Kinoshita N, Utogichi N, Mayumi T, Mizuno N. Int. J. Pharmaceutics. 2004; 286:89.d) Cao B, Reith MEA. Eur. J. Pharmacol. 2002; 448:27. [PubMed: 12126967] e) Erwan S, Samsudin AR, Wihaskoro S. J. Appl. Biomaterials and Biomechanics. 2009; 7:29.e) Wihaskoro S, Erwan S, Samsudin AR, Ibrahim MF. Biomedicine and Pharmacotherapy. 2008; 62:328.f) Robin E, Derichard A, Vallet B, Hassoun SM, Nevriere R. Pharmacological Reports. 2011; 63:1189. [PubMed: 22180361]

25. Pfeiffer S, Leopold E, Hemmens B, Schmidt K, Werner ER, Mayer B. *Free Rad. Biol. Med.* 1997; 22:787. [PubMed: 9119246]
26. Tanno M, Sueyoshi S, Miyata N, Umehara K. *Chem. Pharm. Bull.* 1997; 45:595. [PubMed: 9145498]
27. a) Cheng J, Xian M, Wang K, Zhu X, Yin Z, Wang PG. *J. Am. Chem. Soc.* 1998; 120:10266. b) Zhu X, He J, Li Q, Xian M, Lu J, Cheng J. *J. Org. Chem.* 2000; 65:6729. [PubMed: 11052125]
28. Marletta MA, Yoon PS, Iyengar R, Leaf CD, Wishnok JS. *Biochemistry.* 1988; 27:8706. [PubMed: 3242600]
29. Chen Z, Stamler JS. *Trends in Cardiovascular Disease.* 2006; 8:259.
30. a) Townsend DM, Tew KD, Tapiero H. *Biomed. Pharmacother.* 2003; 57:145. [PubMed: 12818476] b) Hogg N, Singh RJ, Kalyanaraman B. *FEBS Lett.* 1996; 382:223. [PubMed: 8605974] c) Clementi C, Brown GC, Feelish M, Moncado S. *Proc. Nat. Acad. Sci. USA.* 1998; 95:7631. [PubMed: 9636201] d) Keszler A, Zhang Y, Hogg N. *Free Rad. Biol. & Med.* 2010; 48:55. [PubMed: 19819329] e) Wink DA, Nims RW, Derbyshire JF, Chistodulou D, Hanbauer I, Cox GW, Laval F, Cook JA, Krisna MC, Degraff WG, Baker JB. *Chem. Res. Toxicol.* 1994; 7:519. [PubMed: 7981416] f) Gow AJ, Burek DG, Ischiropolous H. *J. Biol. Chem.* 1997; 272:2841. [PubMed: 9006926] g) Williams DLH. *Acc. Chem. Res.* 1999; 32:869. h) Williams, DLH. *Nitrosation Reactions and the Chemistry of Nitric Oxide.* Elsevier; 2004. Chapters 7, 8.
31. Pastore A, Piemonte F, Locatelli M, Russo AL, Gaeta LM, Guilia T, Fedrici G. *Clinical Chem.* 2001; 47:1467. [PubMed: 11468240]
32. Dicks AP, Swift HR, Williams DLH, Butler AR, Al-Sa'doni HH, Cox BG. *J. Chem. Soc. Perkin Trans.* 1996; 2:481.
33. Itoh Y, Ma FH, Hoshi H, Oka M, Noda K, Ukai Y, Kojima H, Nagano T, Toda N. *Anal. Biochem.* 2000; 287:203. [PubMed: 11112265]
34. Katsuda S, Okada Y, Nakanishi I, Tanka J. *Expt. and Mol. Pathol.* 1988; 48:48.
35. Lau HKF. *Atherosclerosis.* 2002; 166:223. [PubMed: 12535734]
36. Murphy MP. *Biochemica et Biophysica Acta.* 1999; 1411:401.
37. Malinski T, Taha Z. *Nature.* 1992; 358:676. [PubMed: 1495562]
38. Geng YJ, Wu Q, Muszynski M, Hansson GK, Libby P. *Arterioscler. Thromb. Vasc. Biol.* 1996; 16(1):19. [PubMed: 8548421]
39. Bivalacqua TJ, Burnett AL, Hellstrom WJG, Champion HC. *Am. J. Physiol. Heart Circ. Physiol.* 2007; 292:H1340. [PubMed: 17071735]
40. Wei LH, Wu G, Morris SM Jr, Ignarro LJ. *Proc. Nat. Acad. Sci. USA.* 2001; 98(16):9260. [PubMed: 11470919]
41. Nishida K, Abiko T, Ishihara M, Tomikawa M. *Atherosclerosis.* 1990; 83:119. [PubMed: 2242092]
42. Ignarro LJ, Buga GM, Wei LH, Bauer LH, Wu G, Soladato P. *Proc. Nat. Acad. Sci. USA.* 2001; 98:4202. [PubMed: 11259671]

Abbreviations

ABH	S-2-amino-6-boronic acid
NO	nitric oxide
NOS	nitric oxide synthase
LDL	low density lipoprotein
SMC	smooth muscle cell
LMW	low molecular weight
DFDNB	1,5-difluoro-2, 6-dinitrobenzene
GSH	reduced glutathione
HASMC	human aortic smooth muscle cell

cpw	cells per well
DAF-FM DA	4-amino-5-methylamino-2',7'-difluorescein diacetate
DAF-FM	4-amino-5-methylamino-2',7'-difluorescein
ROS	reactive oxygen species
2,4-DFNB	2,4-difluoronitrobenzene
2,6-DFNB	2,6-difluoronitrobenzene
DMAC	N,N-dimethylacetamide
NMP	N-methylpyrrolidinone
MTT	(3-(4,5-dimethylthiazole-2-yl)-2,5-diphenyltetrazolium bromide)
cDMSO	cellular dimethyl sulfoxide
LPS	lipopolysaccharide
IFN-γ	interferon gamma
C-PTIO	2-(4-Carboxyphenyl)-4,4,5,5-tetramethylimidazoline-1-oxyl-3-oxide potassium salt
CDCl₃	deuterated trichloromethane
TMS	tetramethylsilane
THF	tetrahydrofuran
PBS	phosphate buffered saline solution
FBS	fetal bovine serum
Eth-1	Ethidium Homodimer-1
CAM	Calcein AM
TLC	thin layer chromatography
RSNO	S-nitrosothiol
GSNO	nitrosated glutathione
i-NOS	inducible nitric oxide synthase
BEC	S-(2-boronoethyl)-L-cysteine
L-NOHA	L-N ^G -hydroxy-L-arginine



Figure 1.
Conversion of L-arginine to nitric oxide and L-ornithine.

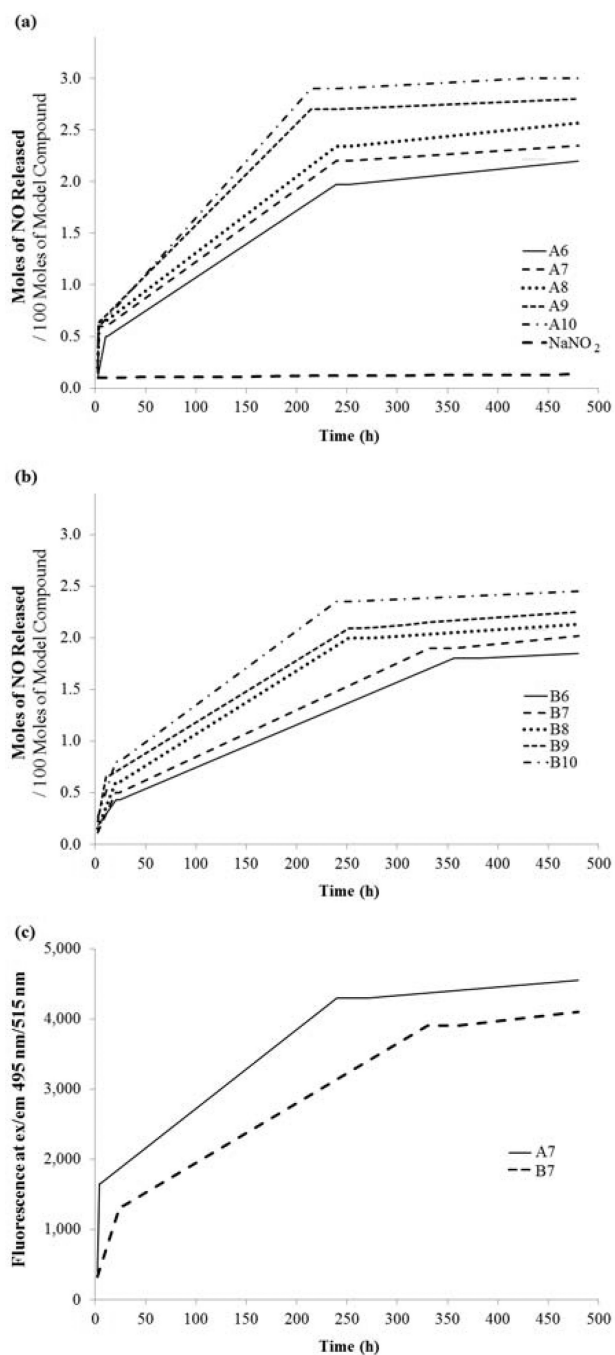


Figure 2.

The release profiles were determined in PBS solution at room temperature using Griess reagent to measure the nitrite concentration produced from the released NO. Absorbance values at 550 nm were determined using a Molecular Devices Plate Reader.

a) NO release profiles of NO-donors, **A6'–A10'**, **b)** NO release profiles of NO-donors, **B6'–B10'**. A fluorescent probe DAF-FM was used as an alternate probe to detect NO and/or N₂O₃. Fluorescent signals were detected using the same micro-plate reader at 495/515 (ex/em) **c)** NO release profiles of **A7'** and **B7'** determined using DAF-FM.

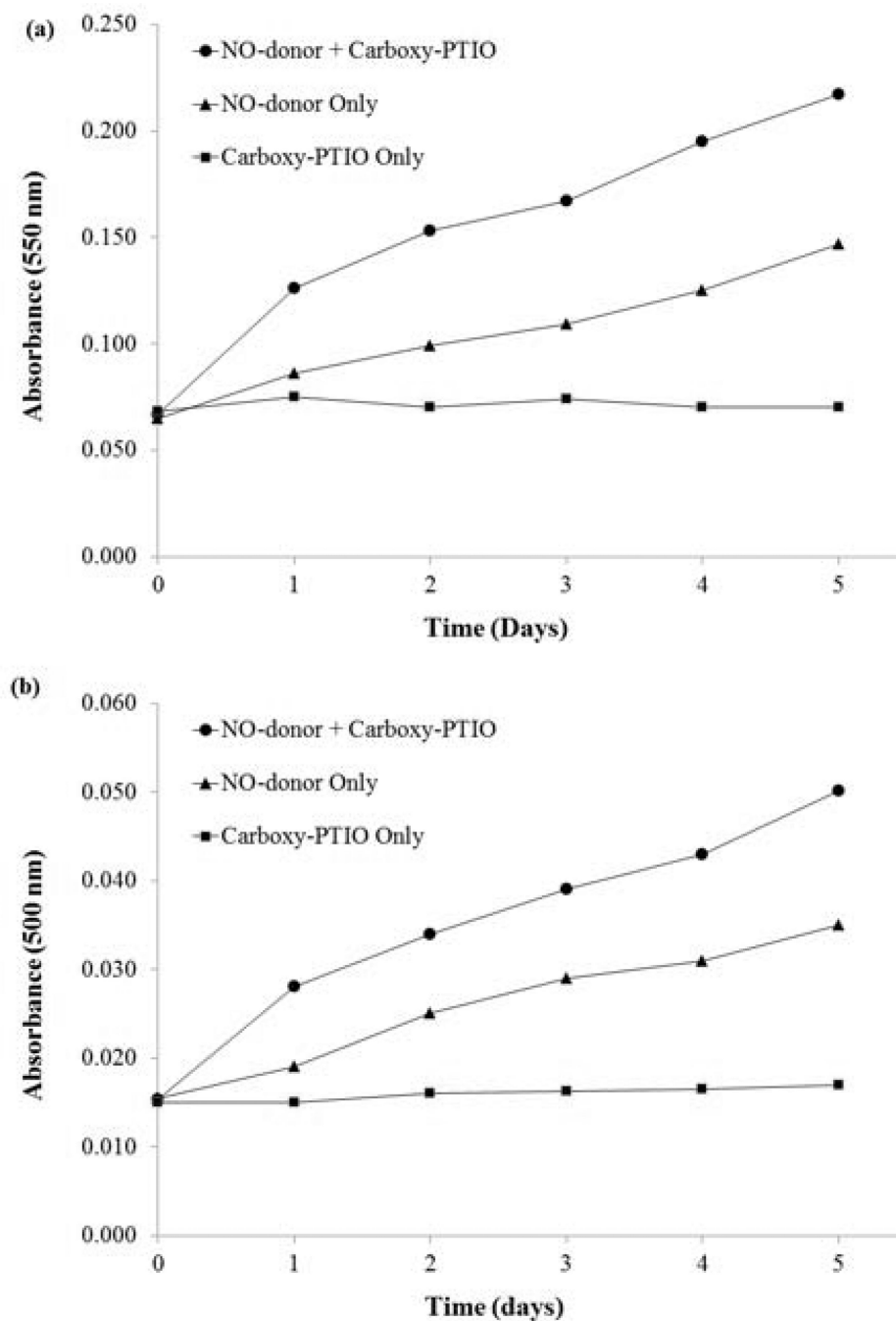


Figure 3.

a) Analyses of nitrite production from NO-donor, **A6'** in the presence and the absence of C-PTIO in 1X PBS. **b)** Analyses of nitrite production from NO-donor, **A6'** in the presence and the absence of C-PTIO in supplemented SMC culture medium. Aliquots were removed every 24 h, treated with Griess reagent and absorbances measured at 550 nm (data displayed in **3a**). Data for **3b** were obtained from absorbances measured at 500 nm with a background subtraction at 630 nm. C-PTIO rapidly captures released NO radical species before a fraction can escape and converts it to nitrite (detected by Griess reagent). Consequently, the presence of C-PTIO results in significantly higher measured nitrite concentrations (higher

absorbance values) than in its absence at any point in time during the span of the experiment (5 days).

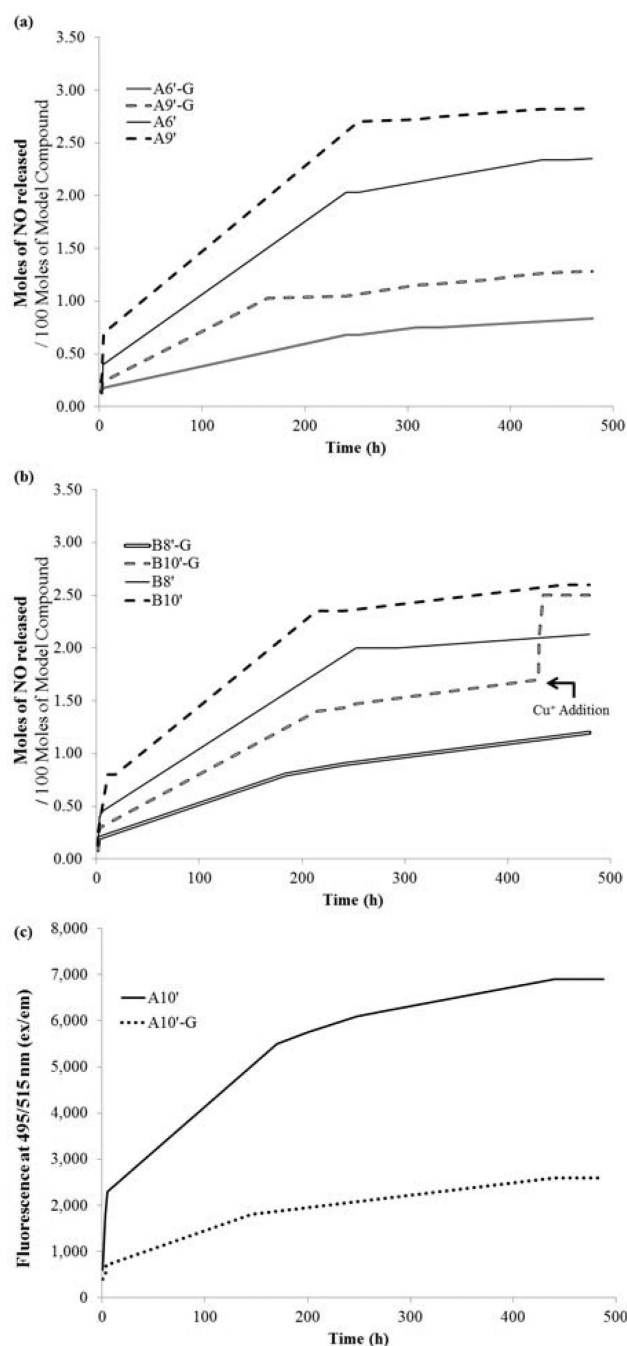


Figure 4.

The release profiles were determined in PBS solution at room temperature using Griess reagent to measure the nitrite concentration produced from the released NO in the presence and absence of GSH. Absorbance values at 550 nm were determined using a Molecular Devices Plate Reader. **a)** NO release profiles of **A6'** and **A9'** in the presence (**A6'G**, **A9'G**) and the absence of GSH (5 mM), determined by Griess reagent **b)** NO release profiles of **B8'** and **B10'** in the presence (**B8'G**, **B10'G**) and the absence of GSH (5 mM). Addition of catalytic amount of Cu⁺ to **B10'G** at t=430 h resulted in the release of NO from GSNO. A fluorescent probe DAF-FM was used as an alternate probe to detect NO and/or N₂O₃.

Fluorescent signals were detected using the same micro-plate reader at 495/515 (ex/em) **c**) NO release profiles of **A10'** in the presence (**A10'G**) and the absence of GSH (5 mM) determined using DAF-FM.

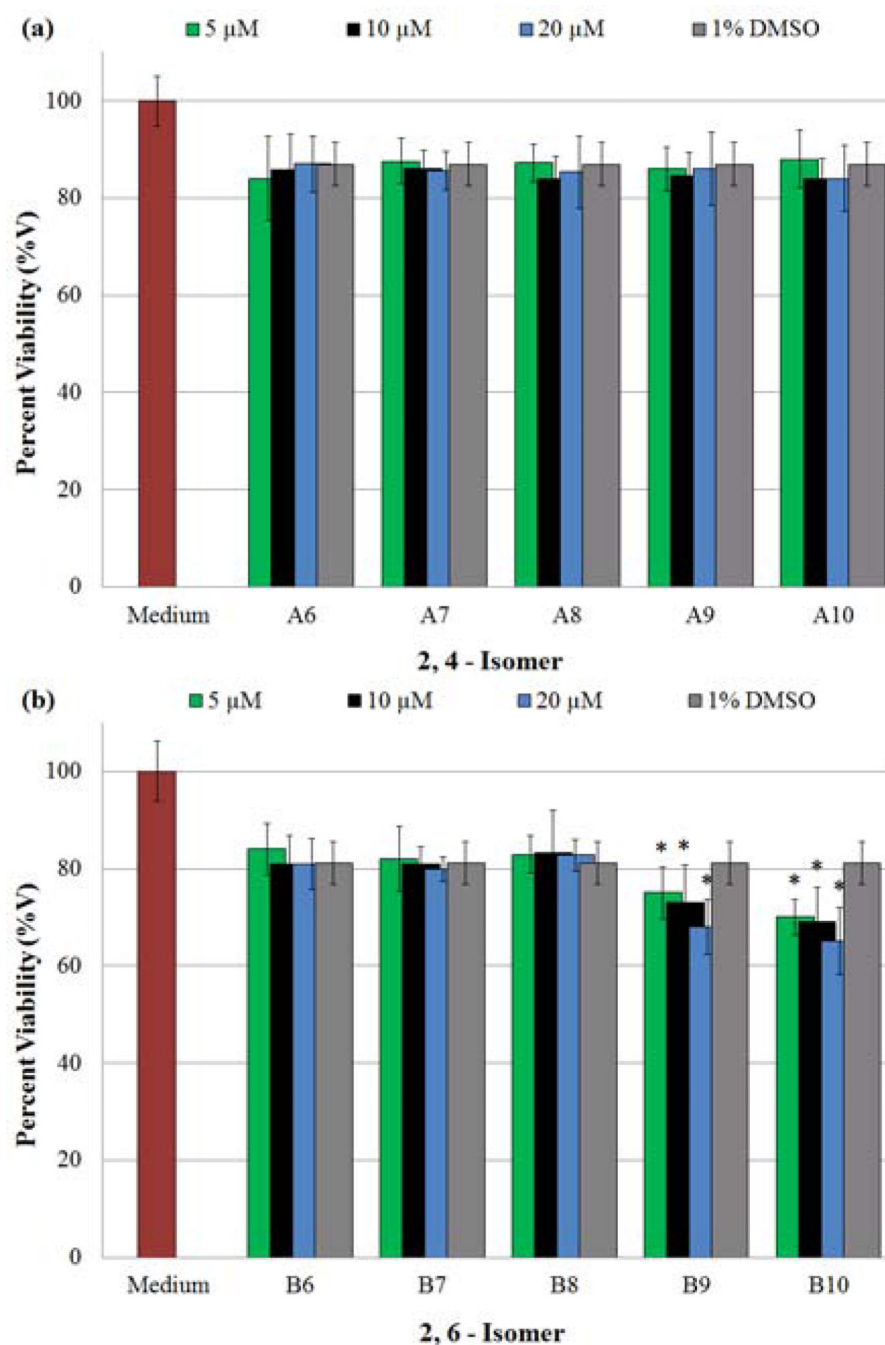


Figure 5. Determination of anti-proliferative effects exerted on cultures of HASMCs by secondary amines. Changes in HASMC proliferation were evaluated using an MTT viability assay, after a 96 h incubation period with a given secondary amine (in cDMSO). Absorbance measurements of each well (570 nm) provided data points, which were expressed as a percentage of the positive control (100%), in which cells were grown in the absence of any test agents. In addition, cDMSO acted as the vehicle to deliver amines; therefore a negative control of 1% cDMSO was also tested for HASMC proliferation inhibition. (*) Indicates a statistically significant difference ($p < 0.05$) between the given compound/concentration combination and the vehicle alone. The graphical data represents the mean \pm SE of triplicate

determinations on the extent of HASMC proliferation inhibition in the presence of **a) A6–A10** and **b) B6–B10**.

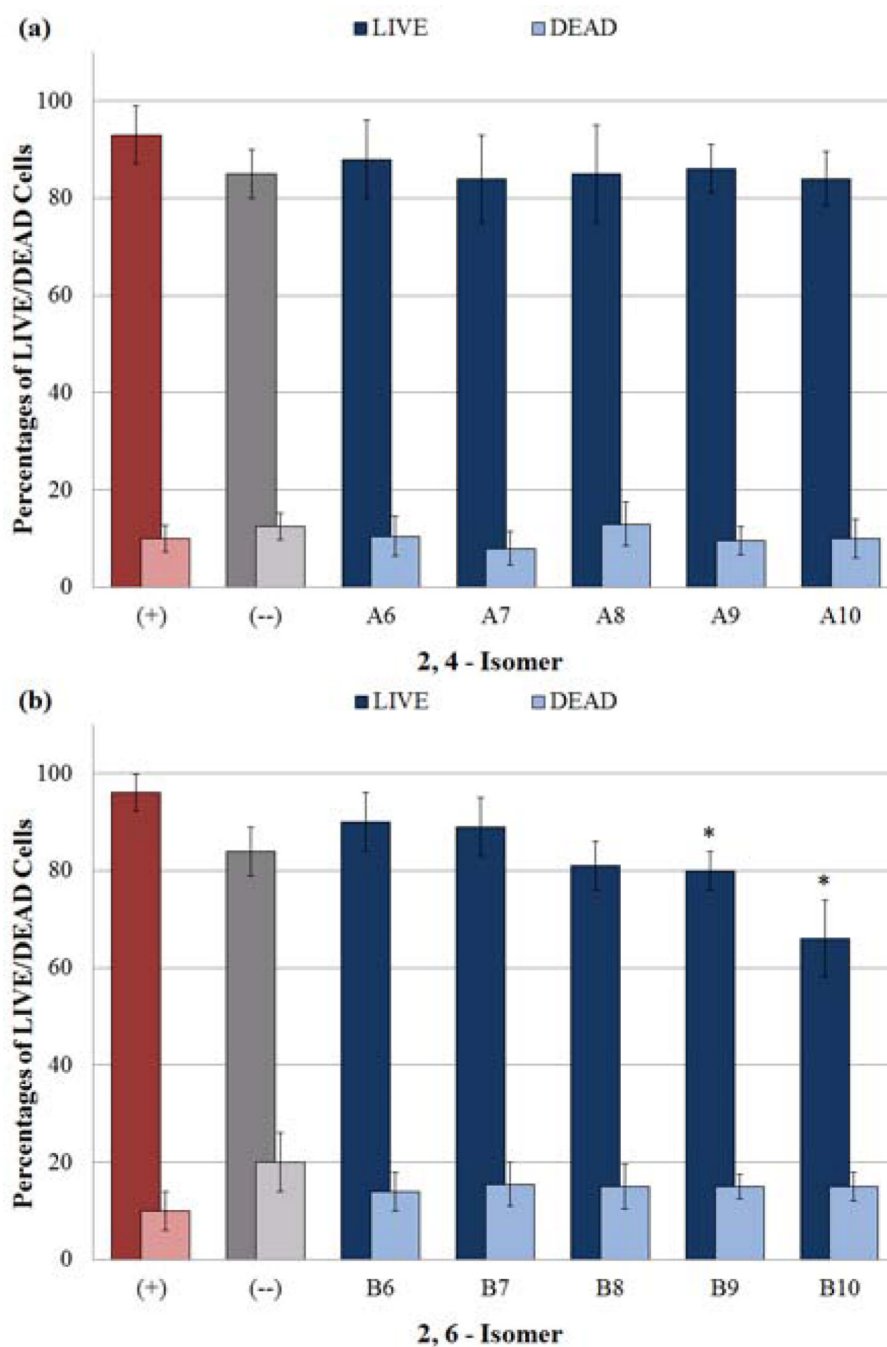


Figure 6. Determination of cytotoxic effects by secondary amines on HASMC cultures using a LIVE/DEAD assay. Two distinct fluorescent measurements at em 495/ex 515 and em 495/ex 635 provided data points for calculating reported percentages of LIVE and DEAD cells respectively. (*) Indicates a statistically significant difference ($p < 0.05$) between the given compound/concentration combination and the vehicle alone. The concurrent decrease in LIVE cells and increase in DEAD cells exhibited by the negative control suggests 1% DMSO induces cell death. Therefore the use of DMSO as the vehicle accounts for the percentage of DEAD cells present in all tested samples. The graphical data represents the

mean \pm SE of triplicate determinations, and reveal the percentages of LIVE and DEAD cells resulting from exposure to **a) A6–A10** and **b) B6–B10**.

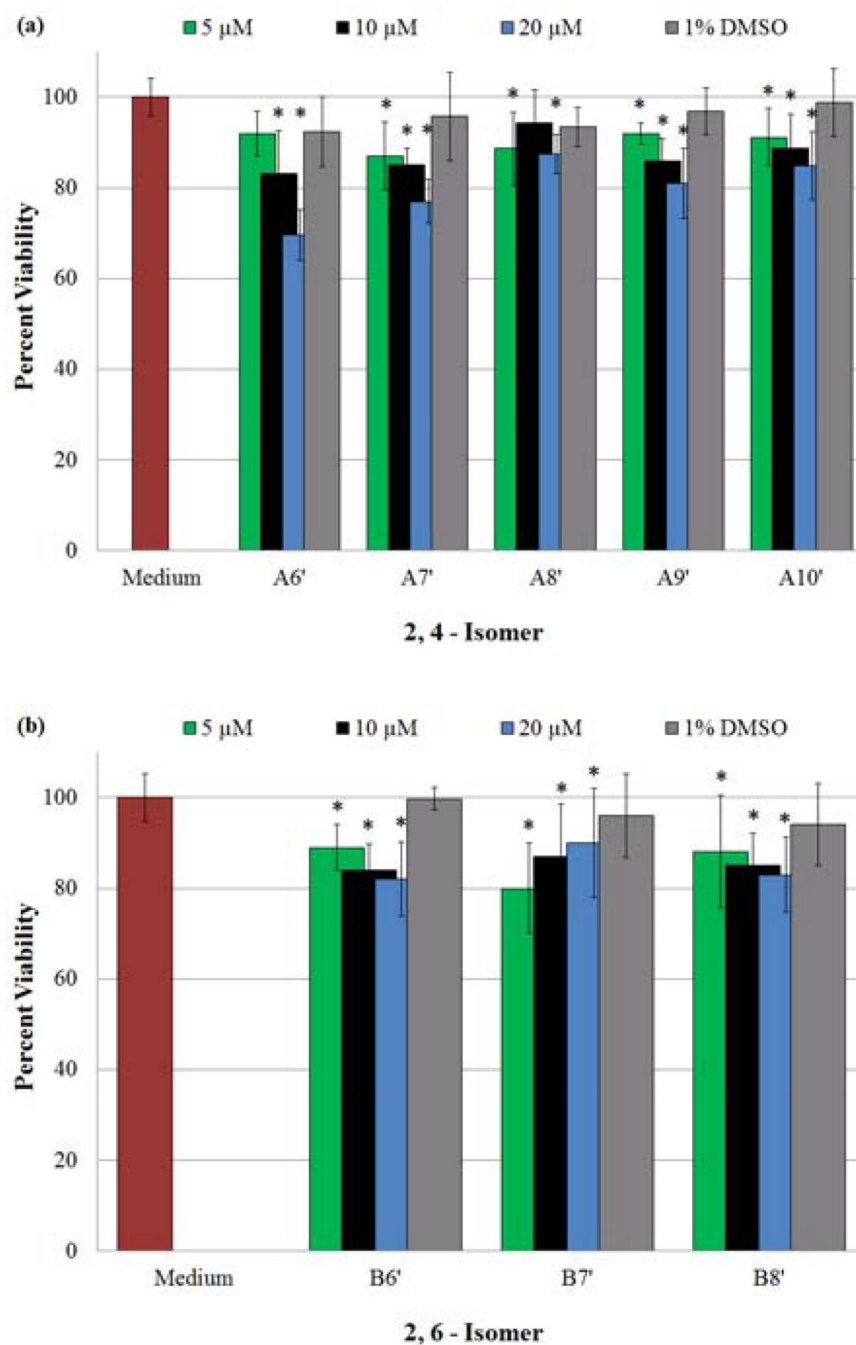


Figure 7. Determination of anti-proliferative effects exerted on cultures of HASMCs by NO-donors, using an MTT viability assay. (*) Indicates a statistically significant difference ($p < 0.05$) between the given compound/concentration combination and the vehicle alone. The graphical data represents the mean \pm SE of triplicate determinations on the extent of HASMC proliferation inhibition in the presence of **a) A6'–A10'** and **b) B6'–B10'**.

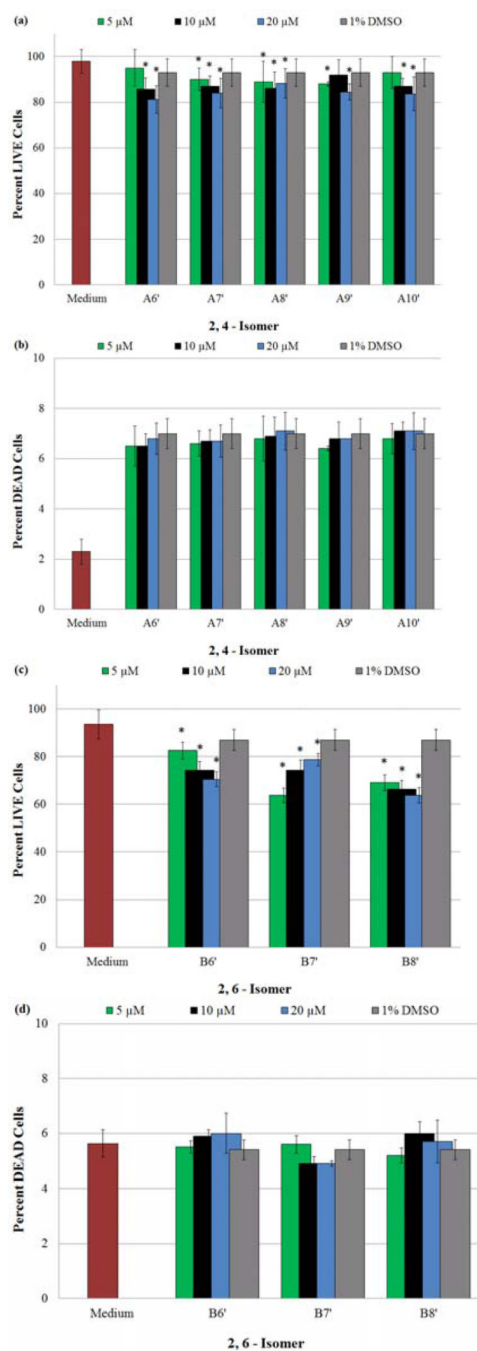


Figure 8. Determination of cytotoxic effects on HASMCs due to presence of NO-donors at varying concentrations, using a LIVE/DEAD assay. (*) Indicates a statistically significant difference ($p < 0.05$) between the given compound/concentration combination and the vehicle alone. A statistically significant decrease in the percentage of LIVE cells, accompanied by no change in the percentage of DEAD cells in the presence of the same compound/concentration combination, verifies a reduction of viable HASMCs due to the inhibition of proliferation. The graphical data represents the mean \pm SE of triplicate determinations, and illustrate **a)** the percentage of LIVE cells after exposure to **A6'–A10'**, **b)** the percentage of DEAD cells after

exposure to **A6'–A10'**, **c)** the percentage of LIVE cells after exposure to **B6'–B10'** and **d)** the percentage of DEAD cells after exposure to **B6'–B10'**.

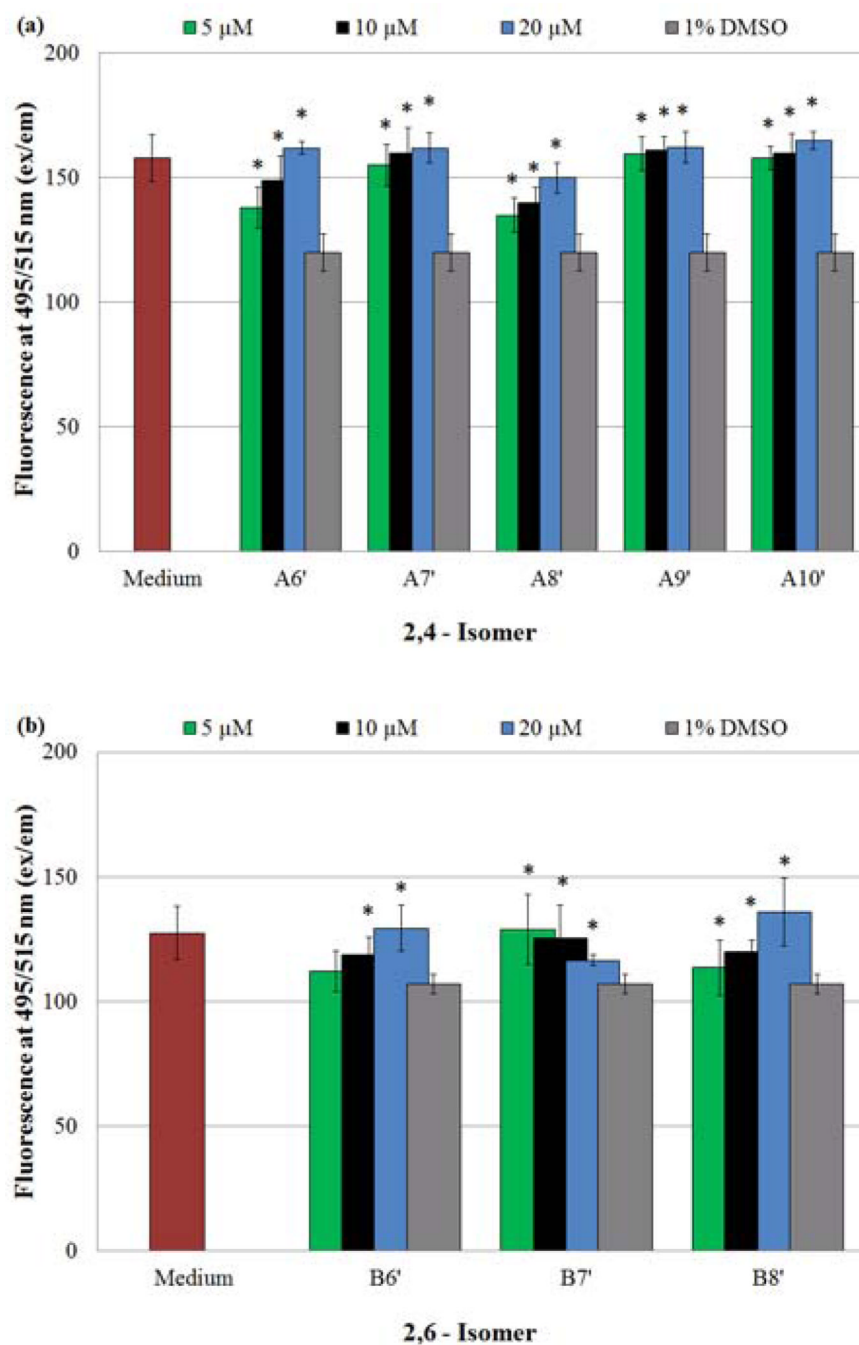


Figure 9. Monitoring of intracellular NO and /or N_2O_3 concentrations of HASMCs exposed to NO-donors, using the membrane-permeable probe DAF-FM DA. Fluorescence measurements (ex 495/em 515) provided data points, which were reported using the given arbitrary units. (*) Indicates a statistically significant difference ($p < 0.05$) between the given compound/concentration combination and the vehicle alone. The graphical data represents the mean \pm SE of triplicate determinations in the presence of a) A6'–A10' and b) B6'–B10'.

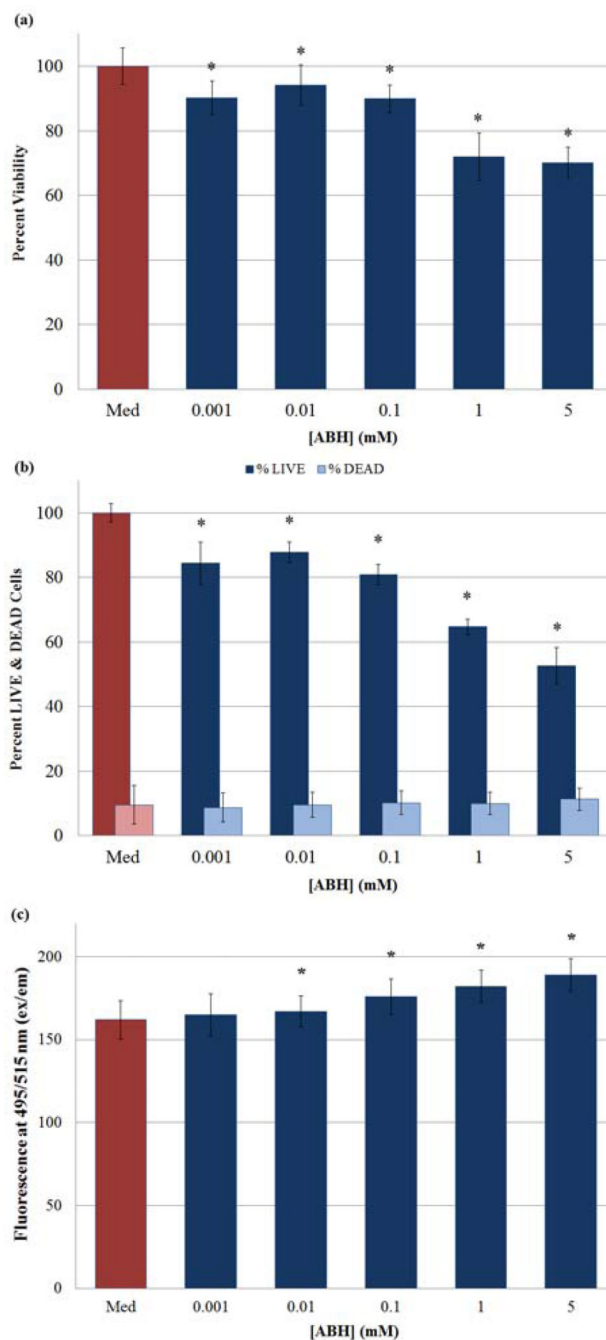


Figure 10. Determination of anti-proliferative and or cytotoxic effects exerted on cultures of HASMCs by ABH at varying concentrations utilizing **a)** MTT Viability Assay and **b)** LIVE/DEAD assay. **c)** Additionally, changes in HASMC intracellular NO and/or N_2O_3 concentrations were determined in the presence of varying ABH concentrations using DAF-FM DA. (*) Indicates a statistically significant difference ($p < 0.05$) between the given compound/ concentration combination and the positive control. The graphical data represents the mean \pm SE of duplicate determinations.

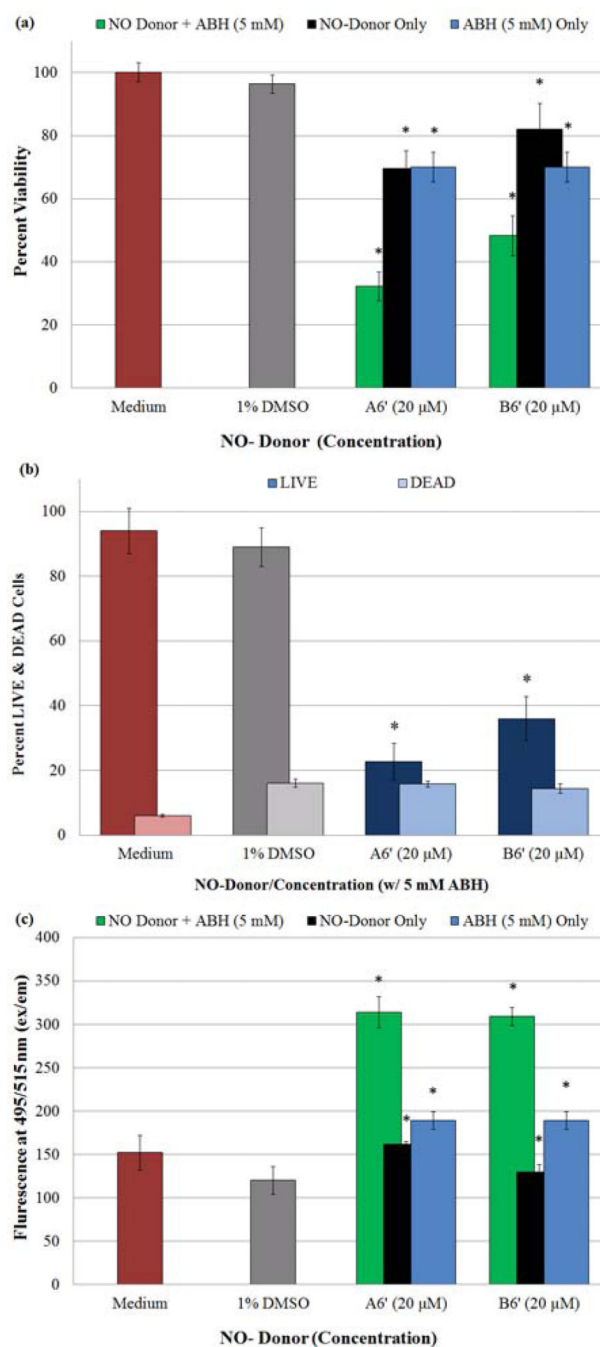


Figure 11.

Determination of anti-proliferative and or cytotoxic effects exerted on cultures of HASMCs by **A6'** (20 μM) and/or **B6'** (20 μM) in combination with ABH (5 mM) utilizing **a**) MTT Viability Assay and **b**) LIVE/DEAD assay. **c**) Additionally, changes in HASMC intracellular NO and/or N₂O₃ concentrations were determined in the presence of **A6'** (20 μM) and/or **B6'** (20 μM) + ABH (5 mM) using DAF-FM DA. (*) Indicates a statistically significant difference ($p < 0.05$) between the given compound/ABH combination and the negative control. The graphical data represents the mean \pm SE of duplicate determinations.

Table 1

Percent Nitrosation, Mole Percentage of Released NO, and Half-lives of NO Donors Prepared from Model Compounds. Profiles obtained in PBS Solution (Top) and in the presence of GSH (Bottom).

Model Compounds	# Carbons	% Nitrosated	NO released (mole %)	Apparent half-life (h)
A6'	6	100	2.34	105
A7'	7	100	2.48	87
A8'	8	100	2.63	83
A9'	9	100	2.83	69
A10'	10	100	3.00	60
B6'	6	100	1.85	140
B7'	7	100	2.02	126
B8'	8	100	2.13	93
B9'	9	100	2.32	80
B10'	10	100	2.60	62
A6'	6	100	0.84	126
A9'	9	100	1.29	109
B8'	8	100	1.32	123
B10'	10	100	1.90	108

Table 2

Extent of HASMC proliferation inhibition exhibited by NO-donors with and without ABH (5 mM)

	A6'	B6'	ABH
Concentration:	20 μ M	20 μ M	5 mM
% Viability Reduction:			28
Without ABH (R_{wo})	23	18	--
Sum reduction ($R_{wo} + R_{ABH}$)	51	46	--
With ABH (R_w)	64	48	--
$R_w - (R_{wo} + R_{ABH})$	13	2	--